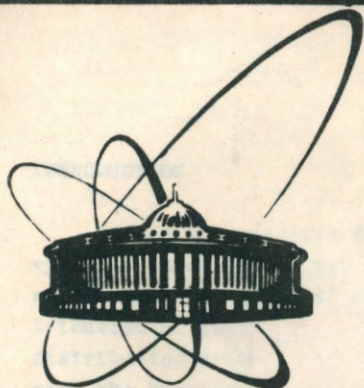


89-249



ОБЪЕДИНЕННЫЙ  
ИНСТИТУТ  
ЯДЕРНЫХ  
ИССЛЕДОВАНИЙ  
ДУБНА

E4-89-249

R.V.Jolos, S.M.Lukyanov, A.K.Nasirov\*,  
V.P.Permjakov, V.S.Salamatin, G.G.Chubarian\*\*

INVESTIGATION OF EFFECT OF NUCLEI SHELL  
STRUCTURE ON MASS DISTRIBUTION  
OF MULTINUCLEON TRANSFER  
REACTION PRODUCTS

Submitted to "Ядерная физика"

\*Institut of Nuclear Physics of Academy  
of Sciences, Uz.SSR.

\*\*Yerevan Physical Institut, Yerevan, Ar.SSR.

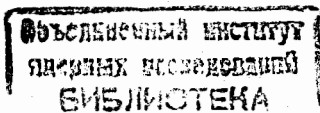
1989

## INTRODUCTION

One of the specific features of deep inelastic collisions of heavy ions, which is not yet supplied with a unique explanation, is a small value (or absence) of the centre shift of the charge (mass) distribution of reaction products at a sufficiently large value of the distribution width. Only at large dissipation of the initial energy, when the kinetic energy of the system decay products is close or even less than the Coulomb repulsion energy (calculated for two adjacent spherical nuclei) one can observe an essential shift of the charge distribution<sup>/1-3/</sup>. This behaviour of the distribution cannot be explained by the diffusion model<sup>/4/</sup> widely used for describing experimental data. The attempt to explain the observed effect has been made in ref.<sup>/5/</sup> by introducing into consideration degrees of freedom arising from formation of a "neck" between nuclei. Absence of the charge distribution shift has been ascribed in ref.<sup>/6/</sup> to equality of the excitation energies of fragments at the initial reaction stage. In the course of establishing thermal equilibrium in a dinuclear, under the influence of temperature difference nucleons go from a light fragment to a heavy one compensating the current of nucleons from a heavy fragment to a light one under the action of strength connected with the potential energy of a dinuclear system. Similar ideas have been developed in the paper by R. Schmidt<sup>/7/</sup> suggesting an auxiliary mechanism of a fast nucleon transfer.

The basic drawback of the above models is their insensitivity or absence of the effect of the nuclear shell structure on the results of calculations. In recent years, more thorough measurements of charge (mass) distribution of products have been performed which need microscopic characteristics of nuclei for analysing the obtained results<sup>/8-10/</sup>.

The role of the shell structure in nuclear reactions at excitation energies  $E^* \leq 40-50$  MeV is very important. The examples are: The width of the charge distribution of products of the  $^{238}\text{U} + ^{208}\text{Pb}$  reaction is larger than in the  $^{208}\text{Pb} + ^{208}\text{Pb}$  reaction<sup>/11/</sup> and in the  $^{238}\text{U} + ^{50}\text{Ti}$  collision is larger than in the  $^{238}\text{U} + ^{48}\text{Ca}$  reac-



tion<sup>/12/</sup> by 15-20% at the same values of the initial kinetic energy loss. This difference is obviously due to the closed proton shells of the nuclei  $^{208}\text{Pb}$  and  $^{48}\text{Ca}$  the number of protons ( $Z$ ) in which is 82 and 20, respectively. A large interval between the last filled and the first unfilled level corresponds to the closed shells, decreases intensity of nucleon exchange. The inclusion of shell corrections allowed one to describe the charge distribution width of the  $^{86}\text{Kr} + ^{197}\text{Au}$  reaction<sup>/13/</sup> products adequately and also the difference in dissipation of the kinetic energy in the reactions  $^{208}\text{Pb} + ^{208}\text{Pb}$ ,  $^{238}\text{U} + ^{238}\text{U}$  and  $^{136}\text{Xe} + ^{209}\text{Bi}$  <sup>/14/</sup>. Another example of the shell structure manifestation is the maximum observed near  $Z = 30$  in the charge distribution of products of the  $^{238}\text{U} + ^{48}\text{Ca}$  reaction<sup>/12/</sup> which is associated with the production of a heavy fragment with  $Z = 82$ , and the maximum at  $Z = 20$  in the differential cross section of the  $^{238}\text{U} + ^{50}\text{Ti}$  reaction. The authors of ref. <sup>/15/</sup> have observed the mass distribution of the  $^{40}\text{Ar}$  (220 MeV) +  $^{241}\text{Am}$  reaction products which has maximal yields of products in the lead and the corresponding co-product. Following theoretical estimations made by Kartavenko<sup>/16/</sup> this picture is a sign of the shells  $Z = 82$  and  $N = 126$  in the nuclear system disintegration.

An increased yield of nuclei in the region of the mass number  $A = 210$  has been observed in studying mass distributions of products of the reactions  $^{48}\text{Ca} + ^{238}\text{U}$ ,  $^{65}\text{Sc} + ^{238}\text{U}$  <sup>/17/</sup>,  $^{40}\text{Ar} + ^{232}\text{Th}$ ,  $^{238}\text{U}$  <sup>/18/</sup>.

The above-mentioned effects indicate the stability of closed shells in the nucleon transfer process in spite of large values of the excitation energy of nuclei.

In the present paper we discuss experimental investigations of the effect of the shell structure of initial nuclei on mass and energy distributions of decay products of a dinuclear system.

#### CONDITIONS OF EXPERIMENT

Experiments were carried out using an external ion beam from the  $\gamma$ -300 accelerator of the Laboratory of Nuclear Reactions, JINR. The products of reactions between the projectiles and target nuclei were recorded by the double-arm time-of-flight spectrometer of which a schematic drawing is shown in Fig. 1<sup>/19/</sup>. The spectrometer is capable of detecting binary products by measuring their velocities and emission angles in a separated plane (in the aperture angle  $\pm 10^\circ$ ) and

outside this plane ( $\pm 5^\circ$ ). On the basis of the measured values two-particle events were selected according to the sum of the particle emission angle in the c.m. system,  $\bar{\theta}_3 + \bar{\theta}_4$ , without any assumptions concerning the reaction mechanism. For events that satisfied the condition of  $\bar{\theta}_3 + \bar{\theta}_4 = 180^\circ \pm 5^\circ$  the values of product masses before nucleon evaporation were calculated.

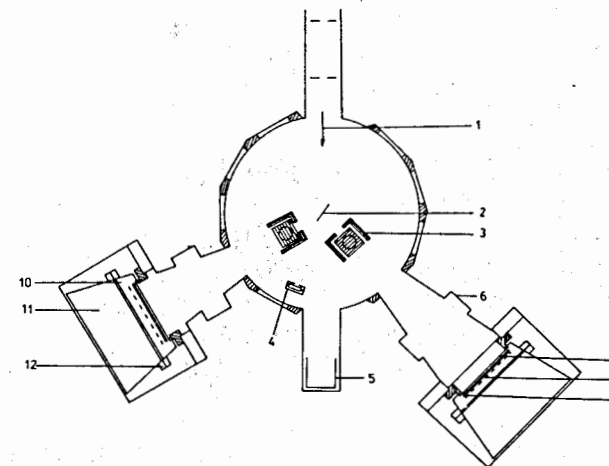


Fig. 1. Experimental setup. A schematic drawing of the double-arm time-of-flight spectrometer: (1) collimator; (2) target; (3) starting detectors; (4) monitor; (5) Faraday cup; (6) path length; (7) entrance window of the ionization chamber; (8) and (9) parallel-plate avalanche counter and screen grid; (10) and (11) ionization chamber anode; (12) coordinate detector in the ionization chamber.

For all the reactions investigated the detection of binary products emitted in the angular range  $35^\circ \leq \theta \leq 70^\circ$  was carried out, corresponding to the detection of the products of, for example, the reaction  $^{40}\text{Ar}$  (220 MeV) +  $^{108}\text{Ag}$  in the angular range between  $50^\circ$  and  $130^\circ$  (c.m. system). Thus, the products were detected in the region

$$\theta_{gr} \leq \bar{\theta} \leq \pi - \theta_{gr},$$

where  $\theta_{gr}$  is the grazing angle at which the ratio of the differential cross section of elastic scattering to the Rutherford cross section is equal to 0.25. By using magic and nearly magic nuclei in the entrance channel an attempt can be made to reveal effects indicating the influence of the shell structure of the colliding nuclei on the evolution of the composite nuclear system. Deeply inelastic transfer

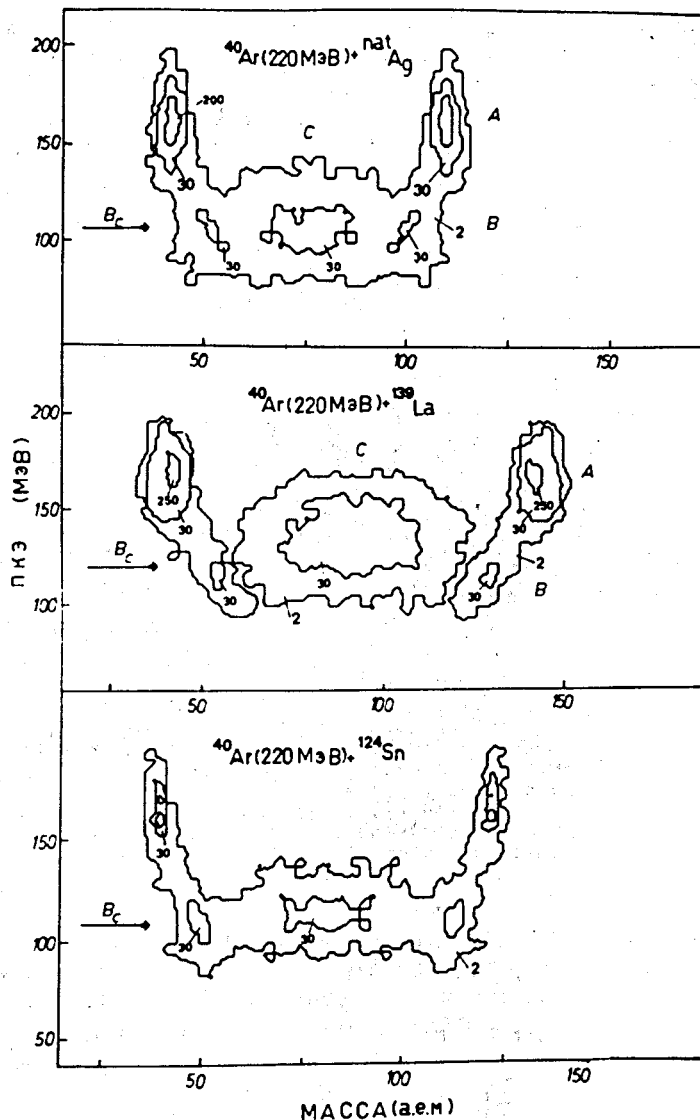


Fig. 2. Results of measuring nuclear yields as functions of the total kinetic energy and product mass in the reactions:  
 (a)  $^{40}\text{Ar}$  (220 MeV) +  $^{108}\text{Ag}$ ; (b)  $^{40}\text{Ar}$  (220 MeV) +  $^{139}\text{La}$ ;  
 (c)  $^{40}\text{Ar}$  (220 MeV) +  $^{124}\text{Sn}$ .

reactions in which the nuclear system does not forget the entrance channel are just the processes which can make it possible to detect the effects of the structure of the initial nuclei. For this purpose the mass and energy distributions were measured of the products from reactions induced by  $^{40}\text{Ar}$  and  $^{64}\text{Zn}$  ions accelerated to about 220 and 315 MeV, respectively, on silver, tin, lanthanum targets.

#### EXPERIMENTAL RESULTS

The experimental studies have demonstrated a qualitative difference between the mass and energy distributions of the products of the reactions  $^{40}\text{Ar} + ^{124}\text{Sn}$ ,  $^{108}\text{Ag}$ ,  $^{139}\text{La}$  and the reactions  $^{64}\text{Zn} + ^{122}\text{Sn}$ ,  $^{108}\text{Ag}$ ,  $^{139}\text{La}$ . In the  $^{40}\text{Ar}$ -induced reactions the maximum of the mass distribution is displaced towards mass symmetry as the total kinetic energy of the products decreases (Fig. 2). In the reactions involving  $^{64}\text{Zn}$  the maximum remains undisplaced until the total kinetic energy of the products were below their Coulomb repulsive energy (Fig. 3). At energies below the Coulomb barrier a second maximum was observed in addition to the quasielastic one. The appearance of the second maximum is likely to be due to the shell stability of the interacting nuclei.

In our view, the observed peculiarities of the mass and energy distributions are accounted for by the shell structure of the nuclei.

#### THE MODEL

As has been mentioned above, the diffusion model using drift and diffusion coefficients independent of charge asymmetry fails to explain the observed specific properties of mass distributions<sup>/20/</sup>. More general is the approach formulated in refs.<sup>/16,21/</sup>. In these papers the consideration is based on the general kinetic equation in which the atomic number of a light fragment  $Z$  at fixed mass number  $A$  is used as a variable:

$$\frac{\partial P_{Z(A)}(t)}{\partial t} = \Delta_{Z+1(A+1)}^{(-)} P_{Z+1(A+1)}(t) + \Delta_{Z-1(A-1)}^{(+)} P_{Z-1(A-1)}(t) - \Delta_{Z(A)} P_{Z(A)}(t),$$

$$\Delta_{Z(A)} \equiv \Delta_{Z(A)}^{(+)} + \Delta_{Z(A)}^{(-)},$$

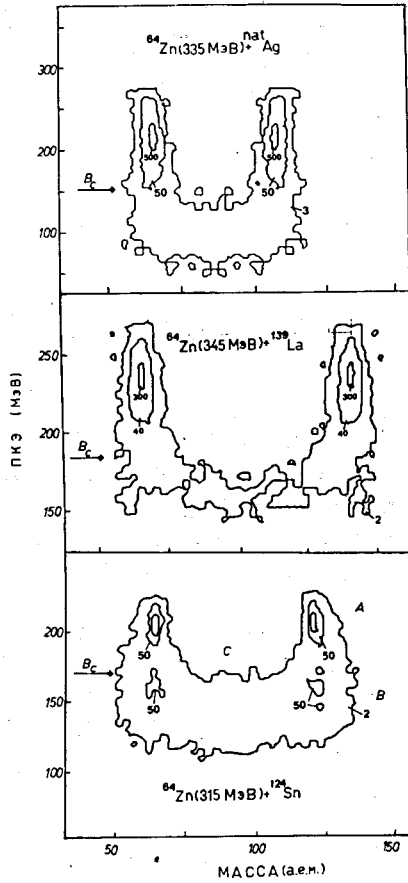


Fig. 3. The same as in Fig. 2 but for the reactions  
 a)  $^{64}\text{Zn}$  (335 MeV) +  $^{108}\text{Ag}$  ;  
 b)  $^{64}\text{Zn}$  (345 MeV) +  $^{139}\text{La}$  ;  
 c)  $^{64}\text{Zn}$  (315 MeV) +  $^{124}\text{Sn}$  .

here  $P_{Z(A)}(t)$  is the probability of finding a dinuclear system at moment  $t$  in the state of charge (mass) asymmetry  $Z(A)$  .

Dependences of macroscopic transition probabilities on  $Z$  have been determined under the assumption that in transferring a nucleon from nucleus to nucleus the dinuclear system may convert into any state allowed by the energy conservation law. It follows from this assumption that  $\Delta_{Z(A)}^{(\pm)}$  are proportional to the square root of the ratio of the state densities  $\rho_{Z(A)}(E^*)$  of the dinuclear system to the charge (mass) asymmetries

$Z(A)$  differing by unity with given total energy

$$\Delta_{Z-1(A-1)}^{(+)} \sim \left( \rho_{Z(A)} / \rho_{Z-1(A-1)} \right)^{1/2}, \quad \Delta_{Z+1(A+1)}^{(-)} \sim \left( \rho_{Z(A)} / \rho_{Z+1(A+1)} \right)^{1/2}.$$

Under this consideration the transition probabilities  $\Delta_{Z(A)}^{(\pm)}$  turn out to be dependent only on the nuclear binding energy and insensitive to other shell effects: level densities near the Fermi level, appearance near the Fermi level of a single-particle level with a large degeneracy, etc.

The approach allowing for these effects has been developed in ref. /22/ and used to derive the following expressions for the transition probabilities

$$\Delta_{Z(A)}^{(+)} = \frac{1}{\Delta t} \sum_{P, T} |\chi_{PT}^{Z(A)}(R)|^2 (2j_P^{Z(A)} + 1)(2j_T^{Z(A)} + 1) n_T^{Z(A)} (1 - n_P^{Z(A)}),$$

$$\Delta_{Z(A)}^{(-)} = \frac{1}{\Delta t} \sum_{P, T} |\chi_{PT}^{Z(A)}(R)|^2 (2j_P^{Z(A)} + 1)(2j_T^{Z(A)} + 1) n_P^{Z(A)} (1 - n_T^{Z(A)}),$$

$$n_i^{Z(A)} = 1 / (1 + \exp((E_i^{Z(A)} - S_{Z(A)}^P) / T)), \quad i = P, T.$$

Here  $P$  and  $T$  are the sets of quantum numbers of the single-particle states of a light and heavy nucleus, respectively;  $j_P$  and  $j_T$  are the angular moments of single-particle states;  $n_P$  and  $n_T$  are the Fermi numbers of occupation of one-particle states (the temperature  $T$  of a double nuclear system is determined by the initial kinetic energy and orbital momentum);  $E_i^{Z(A)}$  - is the energy of one-particle states;  $S_{Z(A)}^P$  is the proton separation energy;  $\chi_{PT}^{Z(A)}(R)$  are matrix elements of transition of a nucleon under the action of a mean field  $U(x, R)$  of the double system between one-particle states  $P$  and  $T$  of colliding nuclei

$$\chi_{PT}^{Z(A)}(R) = \frac{1}{i\hbar} \int_t^{t+\Delta t} d\tau \exp\left[\frac{i}{\hbar} (E_P^{Z(A)} - E_T^{Z(A)})\tau - \Gamma_{PT}\tau\right] \cdot \int d^3x \Psi_T^{Z(A)}(x) U(x, R) \Psi_P^{Z(A)}(x-R).$$

In this expression,  $\Psi_P$  and  $\Psi_T$  represent wave functions of one-particle states. We have here taken account of the damping of the particle-hole excitations induced by their decay into more complicated configurations. The decay widths are parametrized as follows /23/:

$$\Gamma_{PT} = \gamma |E_P - E_T|, \quad \gamma = (0, 3 \div 0, 5) \text{ MeV}.$$

The time interval  $\Delta t$  should be larger than the relaxation time of an average field ( $\sim 10^{-22}$  sec.). With changing  $\Delta t$  from this value to the value of the reaction time specific of deep inelastic collisions, the values of  $\Delta_{Z(A)}^{(\pm)}$  have not almost changed. The quantity  $\Delta_{Z(A)}^{(+)}$  was calculated with the use of the separation energy of nucleons in nuclei ( $Z+1, A+1$ ) and ( $Z_P + Z_T - Z, A_P + A_T - A$ ); whereas

$\Delta_{Z(A)}^{(-)}$ , with the use of separation of nucleons in nuclei ( $Z, A$ ) and ( $Z_p + Z_T - Z + 1, A_p + A_T - A + 1$ ), since in the first case a light fragment absorbs nucleon and in the second case it emits them.

The calculations have shown that the quantities  $\Delta_{Z(A)}^{(\pm)}$  depend both on the single-particle level scheme and on the difference of the nucleon-separation energies in nuclei forming a dinuclear system with a given charge (mass) asymmetry  $Z(A)$ . The influence of the nuclear structure reduces with increasing excitation energy.

An average single-particle potential of the dinuclear system has been determined by the nucleon density folding with an effective Migdal nucleon-nucleon interaction<sup>/24/</sup>.

For a further consideration it is important to establish how the dependence  $\Delta_Z^{(\pm)}$  on the charge asymmetry  $Z$  influences the form of  $P_{Z(A)}(t)$ . As an example we choose the dependence  $\Delta_Z^{(\pm)}$  shown in Fig. 4a. The behaviour of  $P_Z$  will be determined by the initial value of the charge asymmetry  $Z_p$ . If  $Z_p$  is in the region where  $\Delta_Z^{(+)} > \Delta_Z^{(-)}$ , the maximum of the distribution of  $P_Z$  will shift towards larger  $Z$  (Fig. 4b). If  $Z_p$  is in the region where  $\Delta_Z^{(+)} < \Delta_Z^{(-)}$  the maximum of the charge distribution will shift towards smaller  $Z$ .

The position of the charge distribution maximum at large values of the interaction time is governed by two conditions. First, an approximate relation  $\Delta_Z^{(+)} \simeq \Delta_Z^{(-)}$  should hold at this point. Second, in deflecting from this point towards larger  $Z$  the inequality  $\Delta_Z^{(+)} < \Delta_Z^{(-)}$  should hold whereas in deflecting towards smaller  $Z$  the sign of the inequality should be opposite ( $\Delta_Z^{(+)} > \Delta_Z^{(-)}$ ). When  $Z_p$  is near this point, the shift of the distribution maximum is small or is at all absent (Fig. 4c).

Let us consider now how the ratio between the proton separation energies in a light and a heavy fragment influences the nature of the dependence of  $\Delta_Z^{(\pm)}$  on  $Z$ . The results of this analysis are shown in Fig. 5 where the  $^{64}\text{Zn} + ^{122}\text{Sn}$  reaction under three simulated assumptions about the ratio between the proton separation of energies in  $Z_N$  ( $S_1^P$ ) and  $S_N$  ( $S_2^P$ ) is used as an example.

In the first case ( $S_2^P - S_1^P = 3$  MeV), as is seen from Fig. 5a,  $\Delta_Z^{(-)}$  exceeds  $\Delta_Z^{(+)}$  in the whole range of values of  $Z$ . Hence, it follows that the charge distribution maximum will shift towards smaller  $Z$ . In the second case ( $S_2^P - S_1^P = -3$  MeV), the picture becomes opposite (Fig. 5b);  $\Delta_Z^{(+)} > \Delta_Z^{(-)}$ . Provided that  $S_1^P = S_2^P$ , the values of  $\Delta_Z^{(+)}$  and  $\Delta_Z^{(-)}$  become similar.

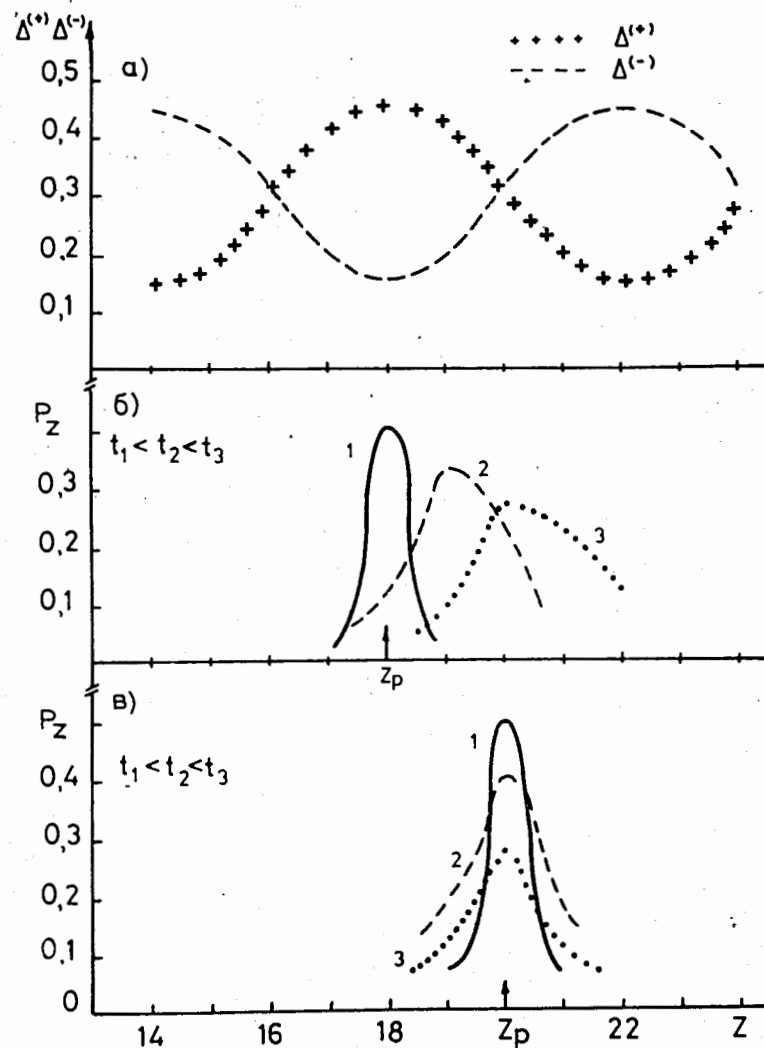


Fig. 4. Relation of the distribution probability of the reaction products  $P_Z(t)$  with the ratio between the matrix elements  $\Delta_Z^{(+)}$  and  $\Delta_Z^{(-)}$ . a) Dependence of  $\Delta_Z^{(+)}$  and  $\Delta_Z^{(-)}$  on the atomic number of a product; b) and c) evolution of the distribution functions  $P_Z(t)$  at different values of the charge asymmetry of the initial channel.

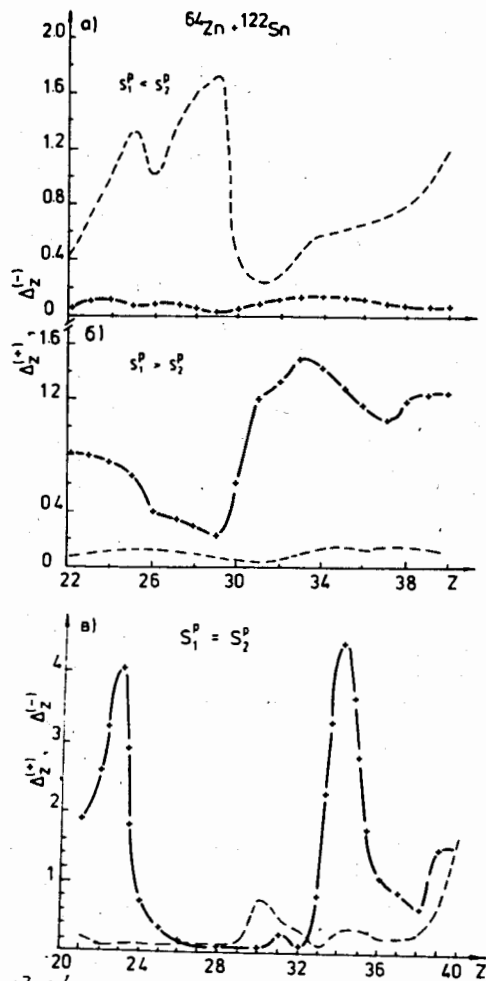


Fig. 5. Dependence of the matrix elements  $\Delta_Z^{(+)}$  (---) and  $\Delta_Z^{(-)}$  (---) on the ratio between the proton separation energies ( $S_p$ ) in colliding nuclei exemplified by the  $^{64}\text{Zn} + ^{122}\text{Sn}$  reaction:

- a)  $S_1^p < S_2^p$  ( $S_2^p - S_1^p = 3 \text{ MeV}$ ),
- b)  $S_1^p > S_2^p$  ( $S_2^p - S_1^p = -3 \text{ MeV}$ ),
- c)  $S_1^p = S_2^p$

#### DISCUSSION OF THE RESULTS

We shall now compare the results of calculations of the mass distributions of products of the  $^{40}\text{Ar}(220 \text{ MeV}) + ^{108}\text{Ag}$ ,  $^{124}\text{Sn}$ ,  $^{139}\text{La}$  and  $^{64}\text{Zn}$  ( $315 \text{ MeV}$ ) +  $^{108}\text{Ag}$ ,  $^{122}\text{Sn}$ ,  $^{139}\text{La}$  reactions with experimental data. In this paper we do not give the whole analysis of experimental data. We did not calculate double differential cross sections

$\frac{d^2\sigma}{dE dZ}$ . Our goal was to elucidate why in reactions with the  $^{64}\text{Zn}$  ions the position of the maximum of charge distribution is independent of the kinetic energy losses (i.e. reaction time) and coincides with the initial value of charge asymmetry. Why in reactions with the  $^{40}\text{Ar}$  ions the position of the charge distribution maximum of light products constantly shifts towards larger  $A$  with increasing to the kinetic energy loss. Experimental data on the energies of proton separation  $S_Z^p$  are taken from the Wapstra table<sup>/25/</sup>. It has also been assumed that the  $N/Z$  - equilibration is established rapidly enough. Besides we take account of the fact that in the reaction isotopes with an even number of neutrons are formed with a large probability.

Since for a fixed  $A$  charge distribution is very narrow<sup>/26/</sup>, the  $A$  and  $Z$  distributions are strictly connected. Therefore the charge distributions calculated in the model<sup>/22/</sup> can be transformed to the mass distributions. In this case proton-shell effects are to be explicitly taken into account. The influence of the neutron shells will manifest itself through noticeable changes of the proton-separation energy  $S_Z^p$  which considerably increases for the nuclei with filled neutron shells  $N = 20, 28, 50, 82$ . In particular isolated maximums have appeared in the calculated charge distributions for isotopes with these neutron numbers.

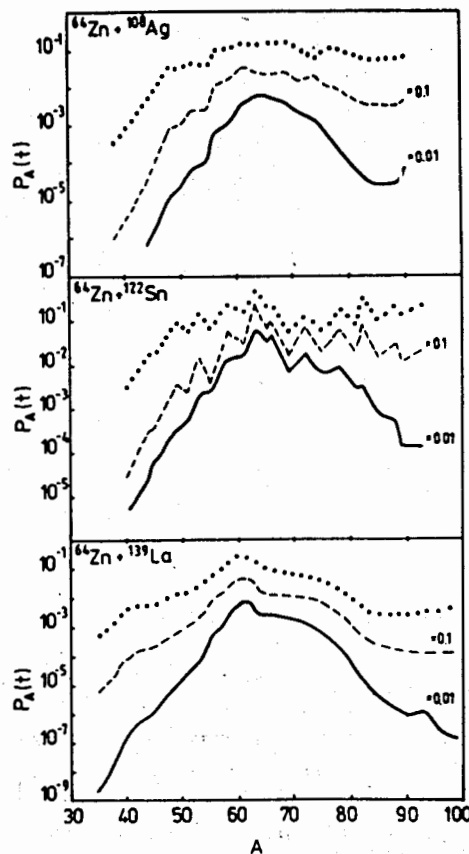
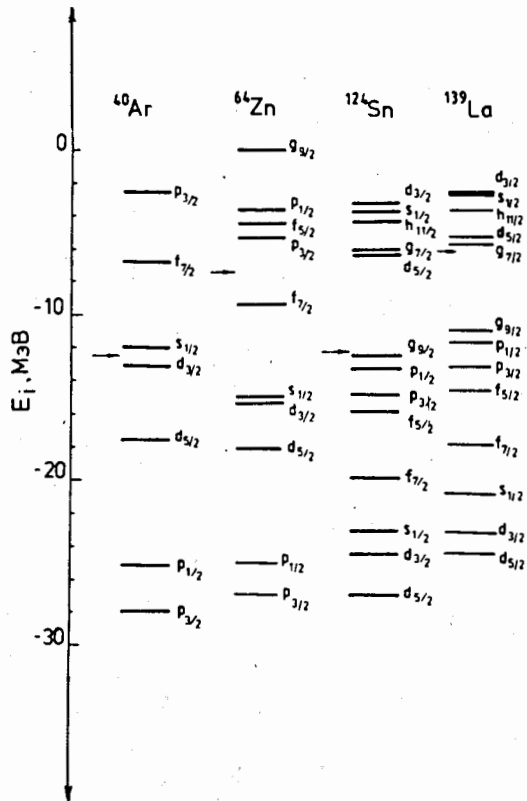


Fig. 6. Probability of the mass distribution of products  $P_A(t)$  versus the reactions  $^{64}\text{Zn} + ^{108}\text{Ag}$ ,  $^{122}\text{Sn}$ ,  $^{139}\text{La}$  for three values of the effective temperature  $T$  and interaction time  $t_{int}$ : —  $T = 0.35 \text{ MeV}$ ,  $t_{int} = 4 \cdot 10^{-22} \text{ c}$ ; ---  $T = 2.0 \text{ MeV}$ ,  $t_{int} = 10^{-21} \text{ c}$ ; ...  $T = 1.5 \text{ MeV}$ ,  $t_{int} = 40 \cdot 10^{-22} \text{ c}$ .

Figure 6 present the calculated probabilities of mass distributions  $P_A(t)$  of products of the reactions  $^{64}\text{Zn} + ^{108}\text{Ag}$ ,  $^{122}\text{Sn}$ ,  $^{139}\text{La}$  for various times of interaction. The smallness or even absence of the mass shift are caused by the shell structure of the  $^{64}\text{Zn}$  nucleus and target nuclei. The  $^{64}\text{Zn}$  superclosed shell  $Z = 28$ , contains two protons in

the state  $P_{3/4}^{127,28}$  (Fig. 7). If, for instance, a light fragment transfers these protons to a target nucleus, it will become very stable relative to the nucleon transfer. At the same time, owing to a rapid set-out of the  $N/Z$ -equilibration, several neutrons from the target nucleus pass over into the light fragment; therefore the mass of the light fragment either changes slightly or does not change at all.

Fig. 7. Scheme of single-particle levels in nuclei  $^{40}\text{Ar}$ ,  $^{64}\text{Zn}$ ,  $^{124}\text{Sn}$ ,  $^{139}\text{La}$ . Arrows indicate the position of the Fermi surface.



Stability of the maximum position of the mass distribution  $P_A$  is also promoted by the shell structure of target nuclei.

The  $^{122}\text{Sn}$  nucleus has a closed proton shell; and the  $^{139}\text{La}$  nucleus, the completely filled state with a large multiplicity of degeneracy.

The assumption of the complete  $N/Z$ -equilibration implies that a part of neutrons go over from the nucleus-target into  $^{64}\text{Zn}$ . This leads to an increase in the proton separation energy in  $\text{Zn}$ , which promotes a further transfer of protons (and a related transfer of neutrons) from a heavy to a light nucleus. In the reaction  $^{64}\text{Zn} + ^{108}\text{Ag}$  at large interaction times this produces a shift of the maximum of the mass distribution towards symmetry, in contradistinction to experiment. Perhaps, it means that the transition of protons from a va-

cant level with a large degeneracy multiplicity  $g_{9/2}$  into  $\text{Ag}$  is rapid enough so that the  $N/Z$ -equilibration has no time to set in. From the mass distribution calculated for the reaction  $^{64}\text{Zn} + ^{108}\text{Ag}$  under the assumption of an incomplete  $N/Z$ -equilibration it follows that there is no shift in the mass distribution maximum, in agreement with experiment.

The results of calculations for the reactions  $^{40}\text{Ar} + ^{108}\text{Ag}$ ,  $^{124}\text{Sn}$ ,  $^{139}\text{La}$  are shown in Fig. 8. So, for the reaction  $^{40}\text{Ar} + ^{124}\text{Sn}$  the proton separation energy is almost the same for both the interacting

nuclei. Like in the reaction  $\text{Zn} + \text{Sn}$ , the  $N/Z$ -equilibration is quickly established throughout the whole volume of the double nuclear system, i.e. a part of neutrons go over from  $\text{Sn}$  into  $\text{Ar}$ . As a result, the proton separation energy in  $\text{Ar}$  grows, the one in  $\text{Sn}$  diminishes, and the proton flow from  $\text{Sn}$  into  $\text{Ar}$  starts to dominate. In  $\text{Sn}$  near the Fermi surface there is a fully occupied level with a large degeneracy multiplicity  $g_{9/2}$ , the nucleon-transition rate from which to  $\text{Ar}$  is higher than in the opposite direction.

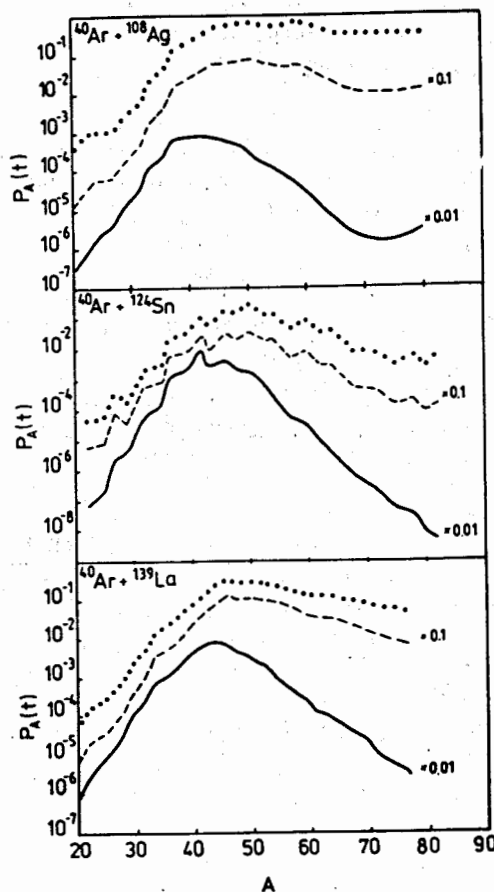


Fig. 8. The same as in Fig. 6, but for the reactions  $^{40}\text{Ar} + ^{108}\text{Ag}$ ,  $^{124}\text{Sn}$ ,  $^{139}\text{La}$ .

In  $^{40}\text{Ar}$  near the Fermi surface there is a vacant level with a high multiplicity of degeneration  $f_{7/2}$ . In the reactions  $^{40}\text{Ar} + ^{108}\text{Ag}$  and  $^{40}\text{Ar} + ^{139}\text{La}$ , the ratios between the proton separation energies in an incident ion and a nucleus-target make the transition of nucleons from a heavy into a light fragment dominant.

Note that if we attempt to interpret experimental data under the assumption that at an early stage of the reaction the excitation energy is equally distributed between nuclei, i.e. a light nucleus is more heated, then the tendency towards increasing charge asymmetry should be more distinct in reactions with Ar ions than in the ones with Zr ions, which contradicts the experiment.

The proposed model was used for interpreting the result of other experiments aimed at studying the dependence of the maximum position of the charge distribution on the kinetic energy loss in the reactions  $^{32}\text{S} + ^{182}\text{W} / 8/$ ,  $^{40}\text{Ca} + ^{238}\text{U}$  and  $^{48}\text{Ca} + ^{238}\text{U} / 10/$ . The calculated results are in good agreement with experimental data.

In the  $^{32}\text{S}$  nucleus unfilled one-particle states  $d_{3/2}$  and  $f_{7/2}$  are as far from the Fermi surface as 6.5 MeV and 9.5 MeV, respectively, which noticeably lowers the transition probability from W to S. As a result, the maximum of the charge distribution shifts towards increasing charge asymmetry with growing kinetic energy losses, i.e. with increasing interaction time.

In the reaction  $^{40}\text{Ca} + ^{238}\text{U}$ , a large density of one-particle states near the Fermi surface in  $^{238}\text{U}$  makes the proton flow from  $^{40}\text{Ca}$  to  $^{238}\text{U}$  dominating. If we change the  $^{40}\text{Ca}$  nucleus to the  $^{48}\text{Ca}$  nucleus, the proton binding energy will increase in an incident ion due to increasing number of neutrons in it, which diminishes the probability of proton transition from the incident ion to the target nucleus. As a result, in the reaction  $^{40}\text{Ca} + ^{238}\text{U}$  the maximum of the charge distribution shifts towards increasing charge asymmetry, whereas in the reaction  $^{48}\text{Ca} + ^{238}\text{U}$  the position of the maximum remains unchanged up to very large kinetic energy losses.

## CONCLUSIONS

Thus, from the observed correlation of the charge-distribution maximum and total kinetic energy of products and its theoretical interpretation within the microscopic model one may infer the importance of consideration of specific features of the structure of colliding nuclei. Strong dependence of the yield of elements of the one-particle-state density near the Fermi surface and on the proton-separation energy points to the nuclei keeping their individuality at the considered excitation energies. Qualitative agreement of the results calculated within the microscopic model<sup>/22/</sup> validates the assumptions underlying the model.

The authors are grateful to Muzychka Y.A. and Pustyl'nik B.I. for useful discussions.

## REFERENCES

1. Schröder W.V. et al. Phys. Report 1978, 45, p. 301.
2. Wozniak G.J. et al. Nucl. Phys. 1983, A402, p. 322.
3. Guarino G. et al. Nucl. Phys. 1984, A424, p. 157.
4. Nörenberg W. Phys. Lett. 1974, B52, p. 289.
5. Grossmann S. and Brosa V.Z. Phys. 1984, A319, p. 327.
6. Moretto L.G. Nucl. Phys. 1983, p. 115c.
7. Schmidt R. Nucl. Phys. 1985, A445, p. 534.
8. Keller J.G. et al. Phys. Rev. 1987, c. 36, No. 4, p. 1364.
9. Schmieder L.M. et al. Phys. Rev. 1988, C37, No. 1, p. 139.
10. Souza R.T. et al. Phys. Rev. 1988, C37, No. 4, p. 1783.
11. Huizenga J.R. et al. Phys. Rev. Lett. 1976, 37, p. 885.
12. Sann H.J. et al. Proc. Int. Workshop on Gross Properties of Nuclei and Nuclear Excitations VI, Austria, 1978, p. 106.
13. Sobotko L.G. Preprint LBL-8519, 1979.
14. Dakowski M. Nucl. Phys. 1982, A378, p. 189.
15. Kalpakchieva R. et al. Nucleonika, 1979, 24, p. 417.
16. Kartavenko V.G. Proceedings of XVI Winter School Bielsko-Biata, Poland, 1978, p. 221.
17. Toke J. et al. Nucl. Phys. 1985, A440, p. 327.
18. Gippner P. et al. Z. Phys. 1986, A325, p. 335.
19. Schilling K.D. et al. Nucl. Instr. and Meth. in Phys. Rev., 1987, A257, No. 2, p. 197.
20. Riedel C.Z. Phys. 1979, A290, p. 47.

21. Moretto L.G. and Sventek J.S. Phys. Lett. 1975, B58, p. 26.
22. Djolos R.V. et al. Yad. Phys., 1986, 44, p. 357.
23. Weidenmüller H.A. In: Progress in Nuclear and Particle Physics, ed. D.H. Wilkinson, Pergamon Press, 1979, p. 88.
24. Migdal A.B. Theory of Finite Fermi-system and properties of atomic nuclei "Nauka", Moscow, 1983 (in Russian).
25. Gareev Ph.A. et al. Physics of elementary particles and atomic nuclei, 1973, vol. 4, part 6, p. 357.
26. Schröder W.V., Huizenga J.R. In: Treatise on Heavy-Ion Science, ed. by D.A. Bromley (Plenum, New York, 1984), vol. 2, chap. 3.
27. Gareev Ph.A. et al. Physics of Elementary Particles and Atomic Nuclei, vol. 4, part. 6, 357 (1973).
28. Ponomarev V.Yu. et al. Nucl. Phys. v. A323, No. 2,3, 446 (1979).

Received by Publishing Department  
on April 11, 1989.

Джолос Р.В. и др.

E4-89-249

Исследование влияния оболочечной структуры ядер на массовое распределение продуктов реакций многонуклонных передач

Приведены результаты измерения двойного дифференциального сечения  $d^2\sigma/dE dA$  в зависимости от массового числа  $A$  и полной кинетической энергии  $E$  продуктов реакций  $^{40}\text{Ar}/220 \text{ МэВ} + ^{108}\text{Ag}, ^{124}\text{Sn}, ^{139}\text{La}, ^{64}\text{Zn}/315 \text{ МэВ} + ^{108}\text{Ag}, ^{122}\text{Sn}, ^{139}\text{La}$ . В рамках микроскопического подхода исследовано влияние особенностей оболочечной структуры сталкивающихся ядер на положение максимума массового распределения продуктов этих реакций. Качественное различие в зависимостях положения максимума от полной кинетической энергии продуктов реакций с  $^{64}\text{Zn}$  и  $^{40}\text{Ar}$ , наблюдаемое в эксперименте, интерпретируется как проявление оболочечной структуры взаимодействующих ядер.

Работа выполнена в Лаборатории теоретической физики ОИЯИ.  
Препринт Объединенного института ядерных исследований. Дубна 1989

Jolos R.V. et al.

E4-89-249

Investigation of Effect of Nuclei Shell Structure on Mass Distribution of Multinucleon Transfer Reaction Products

The double differential cross section  $d^2\sigma/dA dE$  is measured as a function of the mass number  $A$  and total kinetic energy  $E$  for products of the reactions  $^{40}\text{Ar}(220 \text{ MeV}) + ^{122}\text{Sn}, ^{108}\text{Ag}, ^{139}\text{La}$  and  $^{64}\text{Zn}(315 \text{ MeV}) + ^{122}\text{Sn}, ^{108}\text{Ag}, ^{139}\text{La}$ . The effect of specific features of the shell structure of colliding nuclei on the maximum position of the fragment mass distribution is studied within the microscopic approach. A qualitative difference in dependences of the reactions with  $^{64}\text{Zn}$  and  $^{40}\text{Ar}$  observed experimentally points to the shell structure of interacting nuclei.

The investigation has been performed at the Laboratory of Theoretical Physics, JINR.

Preprint of the Joint Institute for Nuclear Research. Dubna 1989